Astron. Astrophys. 335, 467–478 (1998)

ASTRONOMY AND ASTROPHYSICS

Identification of soft high galactic latitude RASS X-ray sources

I. A complete count-rate limited sample*

H.-C. Thomas[1], **K. Beuermann**[2,3], **K. Reinsch**[2], **A. D. Schwope**[4], **J. Trümper**[3], **and W. Voges**[3]

[1] Max-Planck-Institut für Astrophysik, Karl-Schwarzschild-Strasse 1, D-85740 Garching, Germany
[2] Universitäts-Sternwarte, Geismarlandstrasse 11, D-37083 Göttingen, Germany
[3] Max-Planck-Institut für Extraterrestrische Physik, Giessenbachstrasse 6, D-85740 Garching, Germany
[4] Astrophysikalisches Institut Potsdam, An der Sternwarte 16, D-14482 Potsdam, Germany

Received 15 December 1997 / Accepted 31 March 1998

Abstract. We present a summary of spectroscopic identifications for a complete sample of bright soft high galactic latitude X-ray sources drawn from the ROSAT All-Sky Survey which have PSPC count-rates $\mathrm{CR} > 0.5\,\mathrm{cts\,s^{-1}}$ and hardness ratios $\mathrm{HR1} < 0$. Of a total of 397 sources, 270 had catalogued counterparts although most of these were not previously known as X-ray sources; of the remaining 127 sources neither X-ray nor optical properties were previously known. Of the whole sample of very soft X-ray sources 155 were also discovered by the Wide-Field-Camera on board ROSAT. We present spectroscopic identifications of 108 sources and other identifications for further 18 sources; 1 source remains unidentified so far. In practically all cases a unique optical counterpart exists facilitating identification. The largest source classes are AGN, magnetic cataclysmic variables, and hot white dwarfs.

Key words: X-rays: galaxies – X-rays: stars – galaxies: Seyfert – novae, cataclysmic variables – white dwarfs – stars: coronae

1. Introduction

The *ROSAT All-Sky Survey* (RASS) has led to the discovery of about 80.000 X-ray sources above a count-rate of 0.05 cts/s (Voges 1997, Voges et al. 1996a, 1996b, 1998). Identification programs of RASS X-ray sources have been performed by several groups according to different selection criteria, concentrating either on the identification of complete samples in small fields or of bright sources taken from larger areas of the sky (e.g. Burg et al. 1992, Hasinger et al. 1993, Motch et al. 1997a, 1997b, Zickgraf et al. 1997). Optical identifications are rather straightforward for bright sources at high galactic latitudes which usually have a unique optical counterpart on the POSS-I or the UKST survey plates.

In this paper we consider the optical content of the complete sample of the brightest soft RASS sources. The identification of an incomplete extension to fainter sources is reported in paper II of this series. For very soft sources, ROSAT is about a factor of 100 more sensitive than previous X-ray surveys (e.g. Nugent et al. 1983), suggesting a high discovery potential.

The present sample of X-ray sources was selected from the RASS using limits on the count-rate in the Position Sensitive Proportional Counter (PSPC, Pfeffermann et al. 1986) and on the hardness ratio which measure the X-ray flux and the steepness of the observed X-ray spectrum, respectively. Both quanti-

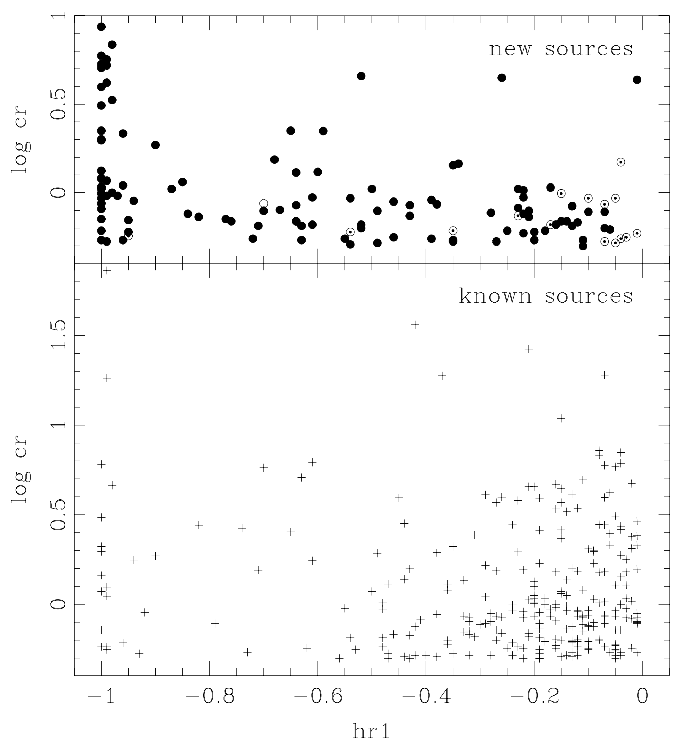

Fig. 1. Distribution of soft RASS sources at galactic latitudes $|b| > 20°$ in the CR−HR1 plane. The *lower panel* shows previously known sources by crosses (+); the *upper panel* shows sources spectroscopically identified in this progam by filled circles (•), sources identified otherwise by dotted circles (⊙), and as yet unidentified sources by open circles (○).

Send offprint requests to: hcthomas@mpa-garching.mpg.de
* Based in part on observations with the ESO/MPI 2.2m telescope at La Silla, Chile

ties depend on the absorbing column density between the source and the observer and, therefore, do not represent intrinsic source properties. Hence, the sources of our sample concentrate in regions of the sky with low integrated Galactic column densities of neutral hydrogen, and the sample is not complete in a physical sense of the source properties.

A few sources which are contained in the *ROSAT All-Sky Survey Bright Source Catalogue (RASS BSC)* (Voges et al. 1996a) and meet our criteria have not yet been identified. Two reasons are responsible for this lack of completeness: (i) Lack of telescope time and (ii) the fact that our program was performed on the basis of information available early in the ROSAT mission which led to the first source catalogue (RASS-I). The reanalysis of the Sky Survey led to the finding of some additional sources (RASS-II, RASS BSC). Count-rates and hardness ratios of individual sources differ somewhat between RASS-I and RASS-II, implying that source selection in terms of CR and HR1 from RASS-I data is not complete in terms of RASS-II data. All values of CR and HR1 quoted here are from the RASS BSC.

A separate identification program covers the entire Galactic Plane at latitudes $|\,b\,| < 20°$ and forms the *Galactic Plane Survey (GPS)* (Motch et al. 1997a, 1997b). The present program covers the complementary latitude range $|\,b\,| > 20°$, but is restricted to the bright sources with soft X-ray spectra. The identification of bright high galactic latitude sources with hard spectra (HR1 > 0) are reported in the ROSAT *Bright Hard Survey* (Hasinger et al. 1997, Fischer et al. in prep.).

2. Bright soft high galactic latitude sources

2.1. Sample definition

The present program aims at the identification of a limited number of the brightest high galactic latitude sources in the RASS which, in addition, have very soft X-ray spectra. A rough measure of the X-ray spectral shape is given by HR1 which is defined in the RASS BSC as HR1 = (HARD-SOFT)/(HARD+SOFT) where SOFT and HARD are the count-rates in the energy bands $0.1 - 0.4$ and $0.5 - 2.0\,\mathrm{keV}$, respectively. HR1 is equivalent to an X-ray "colour" and a negative HR1 implies that $\gtrsim 50\%$ of the counts are detected at $E < 0.4\,\mathrm{keV}$, while for HR1 < -0.6 this percentage rises to $\gtrsim 80\%$. About half of the brighter sources in the RASS BSC have a negative HR1. A manageable number of a few hundred sources to be identified is reached at a count-rate limit of $0.5\,\mathrm{cts\,s^{-1}}$.

Surprisingly, even among the brightest RASS sources a sizeable fraction does not coincide with known objects, represented by e.g. an entry in SIMBAD, the NED, or other available databases; these are termed *unknown* sources. Others do have an entry e.g. in the NED and may, therefore, be considered *known*; however, if the available information was meagre and no spectrum available the source was added to the subset of *unknown* sources. This includes all named galaxies which where not known to house an AGN, for example. Those sources in our sample which were identified by other authors after the survey

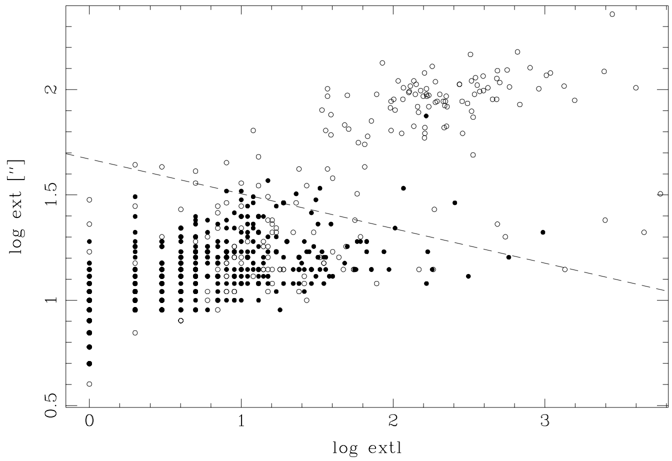

Fig. 2. Measured extent of high galactic latitude RASS sources with CR$>$ $0.5\,\mathrm{cts\,s^{-1}}$ vs. the extension likelihood in a log−log plot. Soft and hard sources with hardness ratios HR1 $<\ 0$ and HR1 $>\ 0$, respectively, are indicated by filled and open circles. The dashed line indicates the approximate division between pointlike (lower left) and truly extended sources (upper right) after Ebeling et al. 1993. There are no truly extended soft sources (see text for discussion).

are included in the *unknown* sample and referenced correspondingly, even if they are catalogued by now. Necessarily, the division between known and unknown sources remains somewhat fuzzy, the intention being to provide more detailed information on those sources whose nature was not known before the RASS.

The nature and properties of the RASS sources with negative HR1 is particularly interesting because previous X-ray missions were not sensitive to this type of sources. We defined our initial sample of sources, therefore, according to the following criteria

– galactic latitude $|\,b\,| > 20°$,
– RASS PSPC count-rate CR $> 0.5\,\mathrm{cts\,s^{-1}}$, and (1)
– hardness ratio HR1 $<\ 0$.

with CR and HR1 taken from the RASS BSC (Voges et al. 1996a). Fig. 1 shows the bright soft high galactic latitude sources split up according to CR and HR1; separately indicated are the *known* sources (crosses), the previously *unknown* sources identified by us spectroscopically (filled circles) or by other means (circles with dot), and the as yet unidentified sources (open circles). The creation of the two subsets of *known* and *unknown* sources is an iterative process which involves both, an analysis of the X-ray properties of individual sources and the search for a plausible optical counterpart. As yet unidentified sources cluster between HR1 $= -0.2$ to 0.0, because in the earlier RASS-I these were assigned HR1 values outside our acceptance window.

A sizable fraction of the bright hard sources is extended and coincides with clusters of galaxies (e.g. Hasinger et al. 1997, Fischer et al. in prep.). In Fig. 2, we show the source extent in arsec as quoted in the RASS BSC vs. the likelihood of extension for all sources with CR$>$ $0.5\,\mathrm{cts\,s^{-1}}$. Soft and hard sources with HR1$<$ 0 and HR1$>$ 0, respectively, are indicated by filled and open circles. Truly extended sources have an extent which roughly exceeds 30 arcsec, somewhat dependent on the likelihood of the fitted extent. A dividing line (Ebeling et al. 1993) separates point-like and extended sources with an uncertainty of 5% to 10%. Thus the number of 8 soft sources well above the line is within the statistical uncertainty of the whole soft sample. Most of the hard extended sources in the upper right of Fig. 2 are clusters of galaxies; all soft sources are compatible with being pointlike. The four soft sources farthest from the dotted line are (sorted by decreasing distance from the line): HR2157/HR2158 (two stars, separation 3′, unresolved), HD 135363 (normal star), GJ 278C (1′ from Castor, unresolved), and WD 1501+664 (white dwarf).

2.2. X-ray analysis

For all sources in the *unknown* subset small photon event tables (PET) where retrieved from the RASS which cover 50×50 arcmin^2 around the respective source. From the PET we derived the source position, the mean PSPC count-rate, the energy spectrum, and the light curve of the source for the time interval covered during the RASS. The derived positions, count-rates, and hardness ratios generally agreed within errors with those quoted (later) in the RASS BSC.

Analysing the PET allowed us to visually inspect the X-ray image for source confusion and structure of the background. Source counts to be used in the light curves and spectra were collected from a circle of 250 arcsec radius around the source position, background counts were taken from a circular region of 400 arcsec radius which was offset from the source position in the scan direction of the satellite and was free of contaminating sources. The light curves and spectra will be discussed elsewhere.

2.3. Optical counterparts

In a first step of the identification program, the source positions were cross-correlated with various catalogues, including, SIMBAD, the NASA/IPAC Extragalactic Database (NED), a collection of X-ray catalogues, the Catalogue of Quasars and Active Galactic Nuclei (7th Edition) (Veron-Cetty & Veron 1996), the Parkes catalogue of radio sources etc. If a plausible known counterpart existed within or very close to the 90% confidence error radius of the X-ray source (see Eq. (2)), the source was considered securely identified and, therefore, *known*. As plausible counterparts we accepted bright stars, particularly of spectral type dM or dK, and bright AGN for sources of intermediate hardness ratios. White dwarfs and AM Herculis binaries are plausible counterparts for the very soft sources with HR1~ -1. In comparing the X-ray and optical positions of stars, the proper motion was taken into account. Ambiguous situations with more than one plausible counterpart ocurred only rarely and are described in the notes to the individual sources given below. A source was considered *unknown* if spectroscopy was needed to clarify its nature. ROSAT sources identified already by other authors are kept in the *unknown* category and referenced accordingly.

In a few cases a normal star coincided with an X-ray source with ultrasoft spectrum (HR1 $\simeq -1$) in which case the X-rays were assumed to originate from a hot white dwarf companion to the normal star; these sources were included in the *unknown* subclass and tabulated as *Spectral type of normal star + WD*, if the white dwarf companion was previously unknown. All but one of these newly discovered binaries are contained in the catalogues of the ROSAT sources detected with the Wide-Field Camera (WFC; Pounds et al. 1993, Pye et al. 1995).

In a second step, we produced finding charts for all doubtful cases and all sources for which no entry in any catalogue was found. We used either the Digitized Sky Survey or the ROE and APM catalogues (Yentis et al. 1992, McMahon & Irwin 1992) of optical objects which are based on scans of the ESO/SERC IIIa-J or the POSS-I red (E) and blue (O) plates, respectively[1]. The doubtful cases included all objects for which the separation exceeded the error radius defined in Eq. (2) or the association of the optical candidate with the X-ray source was not readily acceptable because of an improbable X-ray flux and/or hardness ratio.

In a third step, CCD images and low-resolution spectra were taken of the candidate counterparts of the *unknown* X-ray sources. The southern sources were observed with telescopes at La Silla, Chile, mostly with the ESO/MPI 2.2-m teslesope in MPI time. The northern sources were observed with a variety of telescopes at the Observatoire de Haute-Provence, France, the Calar Alto Observatory, Spain, and the McDonald Observatory, Texas, USA. Spectrophotometry with the ESO/MPI 2.2-m telesope was performed with EFOSC2 in the low-resolution mode (Grism 1) which allowed coverage of the entire range from $3400 - 9200$ Å at 30 Å FWHM resolution. The low-resolution spectra allow a first spectral classification of the counterparts. All AGN and many other sources were subsequently observed at higher resolution which was necessary to determine, e.g. Seyfert subtypes in the case of AGN (Grupe et al. 1998) or the CV subtype (e.g. Beuermann & Thomas 1993). No follow-up higher-resolution spectroscopy was performed for coronal emitters and white dwarfs. CCD photometry and the low-resolution spectroscopy allow us to determine the visual magnitudes of the unknown sources with an accuracy of $0.1 - 0.2$ mag or better.

3. Results and discussion

The combined subclasses of known and unknown sources make up the complete sample of RASS sources with CR$>$ $0.5\,\mathrm{cts\,s^{-1}}$ and HR1$<$ 0. As noted above, the division between known and unknown sources is somewhat arbitrary. Several AGN have been included in the unknown subset if the redshift or the spectral classification was not available, necessitating a spectrum to be taken. In other cases, as e.g. in case of the highly X-ray variable nearby AGN WPVS007 (Grupe et al. 1995b) the object was discovered in a survey of emission line objects (Wamsteker et

[1] We do not reproduce the finding charts here because the DSS can easily be accessed by electronic means, obliterating the need to reproduce the charts in print.

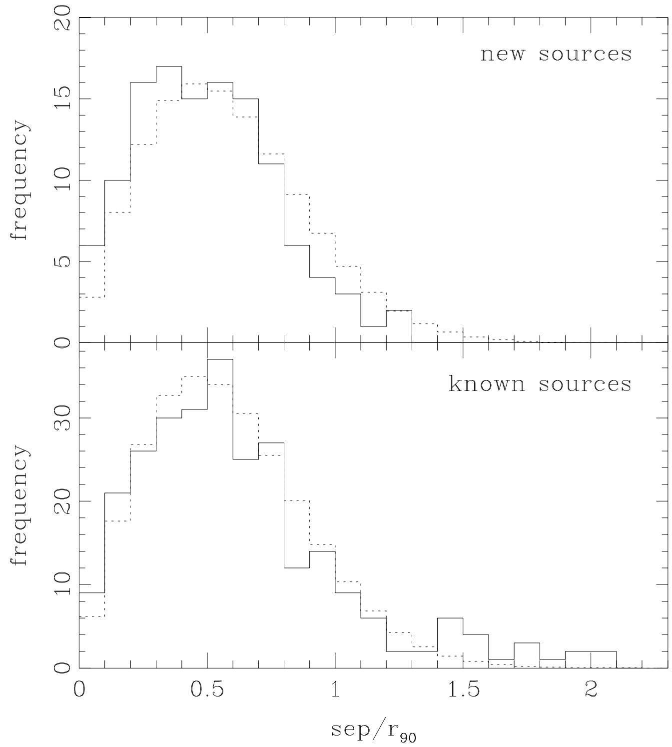

Fig. 3. Normalized separations between optical and X-ray positions in units of the 90%-confidence error radii as given by Eq. 2. *Lower panel:* Known sources; *upper panel:* newly identified sources. The dahed histograms represent Gaussian distributions.

al. 1985) but so little was known about it that inclusion in the unknown category was considered appropriate.

3.1. Known sources

In Table 1, we list the known sources. We used X-ray and optical positions for epoch 2000 taking the proper motion of stars into account. Neither the X-ray positions nor the optical positions are listed here explicitly. The former are available in the RASS BSC (Voges et al. 1996a), the latter are mostly taken from the SIMBAD database with proper motions taken into account where available or from the NED for extragalactic objects. However, we cross-checked all positions with those from the ROE and APM catalogues or the Digitized Sky Survey and if SIMBAD positions were not accurate enough we used those from the sky surveys. The separations between X-ray and optical positions are given in arcsec and in units of the 90% confidence error radius of the X-ray position; this information is used to judge the reliability of the identifications which led to the division between *known* and *unknown* subsets. The 90-% confidence error radius is derived from the 1-σ positional uncertainty Δp given in the RASS BSC:

$$r_{90} = 1.65\,\Delta p \qquad (2)$$

In our sample values for Δp range from 6″ to 35″ with a mean value of 7.5″. Fig. 3 shows the distribution of the normalized

Table 1. Source content of the bright soft high galactic latitude RASS sources, separately for the subsets of *previously known* and *unknown* objects in Tables 2 and 3. For the *unknown* ones the number of sources identified by other means than spectroscopy is given in the third column.

Class	Known	Previously unknown		Total/%
		sp. IDs	inf. IDs	
Coronal emitters	163	13	4	180/45
White dwarfs, PNN	14	17	0	31/8
Star+WD companion	5	7	0	12/3
CV, LMXB, SSS	7	18	2	27/7
AGN (Seyfert, QSO)	64	41	6	111/28
AGN (BL Lac)	17	12	6	35/9
Blank fields				1/0
Total	270	108	18	397/100

separations for the known sources along with a Gaussian adjusted to r_{90} of the known subset. The apparent excess for sep/r_{90} $>$1.4 is caused by stars for which the proper motion may not have been correctly accounted for and by some multiple system which were not resolved by the ROSAT XRT (e.g. 40 Eri ABC). We conclude that for the bright high-galactic X-ray sources considered here a unique and plausible optical counterpart is present in all cases. We expect, therefore, to find unique counterparts also for all or at least most of the previously unknown sources within our CR and HR1 limits.

3.2. Newly identified sources

Table 3 lists the previously unknown sources. Columns 2 and 3 give the optical position, columns 4 and 5 the separation between X-ray and optical positions in arcsec and in units of r_{90} for the individual source, columns 6 and 7 the mean PSPC count-rate and hardness ratio as measured during the RASS and quoted in the RASS BSC, columns $8-11$ give the source class, the type within the class, the redshift if appropriate, and the visual magnitude. Column 12 refers to notes appended to the table. The statistics of the normalized separations between X-ray and optical positions confirms that the proposed counterparts very likely represent the correct identifications. Fig. 3 (upper panel) demonstrates that the separations are in perfect agreement with the uncertainties in the X-ray positions. There is only one source with an unusually large offset, sep$/r_{90} = 4.2$ (not plotted). This source is RX J071506.6–702540 which has a white dwarf as counterpart. Originally thought to be a candidate for a hot isolated neutron star, the pointed PSPC observation (ROR 400321) proved this to be one of the few cases where the RASS position is in error. The pointed PSPC position is 7 arcsec from the white dwarf suggested also by the WFC Consortium as the optical counterpart (Pye et al. 1995).

Spectroscopic identification was not possible for several sources as noted above. In some cases, however, at least the

Table 2. Summary of the optical identification program for previously known sources in our sample ($|b| > 20°$, CR$> 0.5\,\mathrm{cts\,s^{-1}}$, and HR1 < 0). Columns denote (1) the ROSAT name derived from the epoch-2000 X-ray position, (2) the name, and (3) the class of the counterpart, (4) the separation between optical and X-ray positions in arcsec and (5) in units of the 90% confidence radii according to Eq. 2. For names marked with an asterisk a note is added at the end of the table.

(1)	(2)	(3)	(4)	(5)
1RXS J.....	Name	Type	Separ.	
			($''$)	r_{90}
000453.0+343934	HR 9107	G2V	0.8	0.1
000618.9+201215	MRK 335	Sy1	9.1	0.8
000636.8+290112	HR 8	K0V	8.0	0.6
000732.4+331730	GD 2	DA1	6.1	0.5
001208.2–155031	SAO 147143	K0	9.9	0.9
001229.4+143358	LN Peg	K0	13.5	1.2
001354.6–744122	PW And	G6V	11.0	1.0
001821.2+305723	HD 1405	G5	6.1	0.6
002137.3–460526	LHS 5004a	M3	6.0	0.5
002502.7–452941	C17.01	Sy1	8.4	0.6
003452.2–615506	HD 3221	K5V	18.1	1.1
003514.7–033535	BU Cet	F8V	2.5	0.2
004117.7+342513	REJ00412+3425	Ge	9.5	0.8
004248.4+353257	FF And	M0V:e	16.1	1.4
004703.1–115217	NGC 246	PN	4.0	0.3
005307.5–743903	CF Tuc	G3:V+	3.2	0.3
005317.6–325951	WD0050-332	DA1	5.7	0.4
005655.5–515232	BW Phe	K3+K4V	2.3	0.2
005720.4–222300	TON S180	Sy1	5.8	0.4
005837.9–360559	QSO 0056-363	QSO	9.8	0.7
010649.2–225122	CS Cet	G5V	3.9	0.3
011545.7–685221	GJ 55.3AB	F6IV+G5	11.1	0.6
011636.5–023000	AY Cet	G5IIIe	4.0	0.4
011655.2+064841	UV Psc	G5	3.6	0.3
011936.3–282125	QSO 0117-2837	QSO	9.9	0.8
012250.4+004248	BI Cet	G0	7.2	0.6
012256.6+072505	AR Psc	G5	2.2	0.2
013424.0–160708	GD 984	DA	40.7	2.8
013500.7–295430	BB Scl	K3V+K4V	5.2	0.4
013739.7+183525	BD+17 232	K2	9.8	0.9
013853.1+252325	PG 0136+251	DA1p	5.4	0.4
013859.7–175715	UV Cet	M5.5V	10.8	0.8
014100.4–675332	BL Hyi	AM	3.0	0.3
015305.0+293440	alf Tri	F6IV	6.6	0.6
020212.0–623532	HD 12695	F7+F8	0.7	0.1
022232.9–234903	HR 695	G2V	8.7	0.8
022728.4+305828	AG Tri	K5	3.5	0.3
023005.5–085951	MRK 1044	Sy1	2.2	0.2
023438.0–084714	MRK 1048	Sy1	12.0	1.0
023845.4–525710	SAO 232842	K5	8.9	0.7
023901.2–581112	GJ 1049	M0Ve	1.4	0.1
024126.0+055923	BD +05 378	M	14.6	0.9
024240.9–000046	NGC 1068	Sy1	4.4	0.4
024506.5–183416	HR 818	F5+F6V	10.1	0.7
024807.9–365857	HD 17576	G0V	2.8	0.2
024843.0+310701	VY Ari	K0	8.0	0.7
025153.5–613704	VZ Hor	K1Vp	7.1	0.6
025232.3–124610	EP Eri	K1V	7.6	0.7
030242.6–074113	HR 917	K0II-	8.0	0.4
030326.3–240717	PKS 0301-243	BL	4.8	0.4
030755.6–281310	GJ 1054A	K7V	17.7	1.5
030807.1–244539	AE For	K4	15.8	1.2
031203.9–285924	HR 963	F8IV	5.3	0.4
031413.7–223533	EF Eri	AM	12.2	1.1
031920.8+032217	HR 996	G5Vvar	11.3	1.0
032406.6+234714	GJ 140AB	M0V	7.5	0.6
032502.4–415426	ESO 301-13	Sy1	14.8	1.1
032635.1+284302	UX Ari	G5IV	7.0	0.7
032813.8+040945	SAO 111210	K0	15.3	1.0
033256.4–092727	eps Eri	K2V	2.9	0.2
033339.6–370656	0331-373	Sy1	6.0	0.5
033647.2+003518	V711 Tau	G9V	2.3	0.2
034850.1–005823	WD 0346-01	DA2	6.7	0.5
035025.0+171455	V471 Tau*	K2V+DA	10.8	0.9
035141.3–402803	FRL 1116	Sy1	5.3	0.4
040001.9–290205	HD 25284	K0	23.0	1.8
040236.8–001556	HR 1249	F5V	10.0	0.9
040501.1–371110	CTS 44	Sy1	10.7	0.8
040729.6–523413	AG Dor	K1Vp	5.9	0.4
040940.8–075327	EI Eri	G5IV	6.5	0.6
041521.5–073843	40 Eri ABC*	K1V+DA+M5e	26.9	2.0
041527.3+061137	V891 Tau	G5IV	32.8	2.0
042620.9+153646	V777 Tau	F0V	20.1	1.8
043039.9–533656	FRL 303	Sy1	0.9	0.1
043737.3–022937	StKM 1-497	M1	18.1	1.6
043746.1–011930	StHA 32	C1	25.2	1.9
044033.9–415142	HR 1502	F2V	7.1	0.6
044122.7–270811	H 0439-272	Sy1	11.0	0.7
044950.6+065736	HR 1543	F6V	9.0	0.8
045330.2–555128	GJ 2036AB	M2Ve+MV:e	19.7	1.3
045935.4+014701	V1005 Ori	M1	7.3	0.6
050649.5–213505	BD -21 1074	M2	4.7	0.4
052844.7–652700	AB Dor	K1III	3.4	0.3
054334.5–682218	CAL 83	SSS	7.5	0.8
054513.1–595527	XZ Pic	G5	1.7	0.2
060433.0–450312	HR 2157,2158	G0IV+F4V	21.1	1.4
061709.6–371515	HR 2265	A3V	4.4	0.4
061828.8–720242	AO Men	K3:V:	2.8	0.3
062230.9–601301	HD 45270	G1V	9.0	0.8
063800.7–613156	HR 2468	G1.5V	3.9	0.4
073157.1+361340	BL Lyn	M4	8.5	0.7
073437.2+315223	YY Gem	M1Ve	13.7	1.4
080813.8+210612	BD +21 1764	K5+M:	13.0	1.0
080855.4+324908	GJ 1108AB	M.5V+M3V	12.0	0.8
083137.6+192339	CU Cnc	M5e	5.6	0.5
083912.0+650118	HR 3391	G1.5Vb	3.9	0.3
084548.9+485241	HD 74389 AB	A2V+DA	11.0	0.7
085312.3–074312	HD 75997	G5	8.7	0.7
085855.4+082825	G 41-14	M3.5	12.6	1.0
090038.2+414702	GJ 332AB	F3V+G5V	4.9	0.4

Table 2. (continued)

(1) 1RXS J.....	(2) Name	(3) Type	(4) Separ. ($''$)	(5) r_{90}
090326.8+375032	HD 77407	G0	4.7	0.4
092226.2+401213	BF Lyn	K2V	5.9	0.6
092512.3+521716	MRK 110	Sy1	4.8	0.5
092909.4–024552	HR 3759	F6V	18.5	1.4
093036.5+103603	HD 82159	G5	9.9	0.8
093225.5–111101	LQ Hya	K0Ve	3.8	0.3
093243.9+265924	GJ 354.1	K0V:	2.8	0.2
093346.5+624943	FF UMa	G5	3.5	0.3
095652.4+411524	QSO 0953+415	Sy1	3.2	0.3
100002.3+243313	DH Leo	K0V	8.0	0.8
100421.0+502318	G 196-3	K:	13.2	1.1
100811.5+470526	RXJ10081+4705	BL	6.3	0.6
101303.2+355131	TON 1187	Sy1	9.1	0.8
101419.3+210437	DK Leo	M0V:	3.5	0.3
101504.3+492604	GB 1011+496	BL	3.2	0.3
101912.1+635802	MRK 141	Sy1	8.5	0.6
101936.3+195215	AD Leo	M4.5Ve	24.2	1.8
102531.2+514039	MRK 142	Sy1	14.1	1.4
103438.7+393834	Z 1031.7+3954	Sy1	5.1	0.5
105135.3+540438	EK UMa	AM	2.2	0.2
105544.0+602810	DM UMa	K0	3.3	0.3
110425.6+450319	AN UMa	AM	5.4	0.5
110427.1+381231	MRK 421	BL	0.8	0.1
110441.4–041315	HD 96064	G5	0.7	0.0
111238.8+240909	TON 61	DA2	7.8	0.6
111811.1+313154	HR 4374+4375	F8V+G0V	4.0	0.3
111830.0+402557	QSO 1115+407	Sy1	5.0	0.4
111908.1+211915	QSO 1116+215	Sy1	10.2	0.8
112047.5+421217	EXO11180+4228	BL	16.4	1.4
112126.6–202705	GJ 425AB	K5V+M3	7.1	0.5
112756.0+443404	HD 99607	F0	6.2	0.5
113105.2+685156	EXO 1128+691	Sy1	7.2	0.7
113108.9+311409	B2 1128+31	QSO	6.7	0.6
113155.7–343632	CD-33 7795	M2.5Ve	7.0	0.5
113249.2+121022	SAO 99656	G5	3.8	0.3
113626.6+700932	MRK 180	BL	4.0	0.4
113724.4+472752	GJ 9369	K4V	8.4	0.7
113849.7+574245	SBS 1136+579	Sy1	3.4	0.3
113913.6+335552	Z1136.6+3412	Sy1	2.4	0.2
114116.2+215624	WAS 26	Sy1	2.4	0.2
114429.9+365314	CASG 855	Sy1	6.3	0.6
120114.3–034040	MRK 1310	Sy1	1.2	0.1
120308.9+443155	NGC 4051	Sy1	6.7	0.7
120441.9+275417	GQ Com	Sy1	6.5	0.6
120824.6–244336	HR 4623	F0IV/V	7.3	0.6
120946.0+321702	RXJ12097+3217	Sy1	9.1	0.4
121417.7+140312	PG 1211+143	Sy1	1.0	0.1
121723.7–210324	UV Crv	K1V	5.9	0.5
121752.1+300705	B2 1215+30	BL	4.2	0.4
121827.0+294853	MRK 766	Sy1	7.2	0.7
122906.5+020311	3C 273.0	Sy1	4.2	0.4
123004.7–132334	HR 4758	G1+G2V	2.3	0.2
123203.6+200930	MRK 771	Sy1	0.7	0.1
123645.3+475530	PG 1234+482	DA	6.2	0.5
123741.4+264229	IC 3599	Sy2/HII	2.9	0.3
123939.6–052035	MRK 1330	Sy1	5.0	0.4
124139.7–012706	HR 4825	F0V	9.0	0.7
124211.3+331703	WAS 61	Sy1	4.2	0.4
124312.5+362743	GB 1240+3644	BL	4.9	0.4
124635.2+022155	PG 1244+026	Sy1	12.9	1.1
124818.9+582031	PG 1246+586	BL	2.1	0.2
124839.3+601913	HR 4867	F5V	2.0	0.2
125702.4+220155	GJ 153	DA1	5.8	0.6
125731.7+241245	1ES 1255+244	BL	5.7	0.5
125740.2+351334	GJ 490 AB	M0Ve+M4Ve	11.8	1.0
130047.2+122224	DT Vir	M2	13.7	1.0
130947.1+081949	PG 1307+085	Sy1	1.5	0.1
130959.3+173136	HR 4968	F5V	8.1	0.7
131603.0–054000	HD 115247	F8	6.3	0.6
131621.4+290555	HZ 43	DA1	9.2	0.9
131646.6+092530	HR 5011	G0Vs	5.2	0.4
132349.9+654148	PG 1322+659	Sy1	1.9	0.2
132511.6–110932	alf Vir*	B1III+B2V	8.1	0.6
133443.7–082036	EQ Vir	K5Ve	11.3	1.0
133447.5+371100	BH CVn	F2IV	3.8	0.4
133718.8+242306	QSO 1334+246	Sy1	2.0	0.2
134104.8+395942	RXJ13410+3959	BL	3.8	0.3
134356.7+253845	TON 730	Sy1	7.1	0.5
134716.2+172733	HR 5185	F6IV	9.9	0.8
140503.9+100055	HD 123034	G5	6.3	0.6
140516.3+255536	PG 1402+261	Sy1	2.4	0.2
141420.9–152111	MV Vir	K4V	8.8	0.7
141600.9–055955	HR 5338	F7IV	3.1	0.2
141759.6+250817	NGC 5548	Sy1	4.0	0.4
142239.1+580159	RXJ14226+5801	BL	4.1	0.4
142404.3–002656	Q 1421-0013	QSO	9.2	0.7
142725.3+194954	MRK 813	Sy1	4.7	0.4
142832.6+424028	H 1426+428	BL	7.1	0.7
143104.8+281716	MRK 684	Sy1	2.4	0.2
143859.9+641731	EK Dra	F8	1.8	0.2
144207.7+352632	MRK 478	Sy1	9.3	0.9
144248.5+120042	1ES 1440+122	BL	3.6	0.3
145108.5+270933	PG 1448+273	Sy1	7.2	0.6
145123.1+190606	HR 5544	G8V	1.8	0.1
150209.2+661220	WD 1501+664	DZ1	8.1	0.8
150348.3+473924	GJ 575AB	G1+G2	12.4	1.3
150401.5+102620	MRK 841	Sy1	6.0	0.5
150757.9+761214	HD 135363	G5	14.9	1.5
150759.8+041511	SAO 120855	K0	10.0	0.8
152153.0+205830	BPM 90688	M0Ve	8.1	0.6
152918.4+802658	HR 5829	G0IV	11.2	1.0
155909.5+350144	MRK 493	Sy1	3.2	0.2
160141.2+664811	AG Dra	K1	3.1	0.3
160147.7+512053	EK Dra	G5	3.6	0.3
160153.9+583352	HR 5986	F8IV	2.6	0.3
161357.0+654313	MRK 876	Sy1	4.2	0.4
161705.1+551615	CR Dra	M1Ve	9.9	1.0
161955.3+394223	HR 6091	F3IV-V	7.7	0.7

Table 2. (continued)

(1) 1RXS J.....	(2) Name	(3) Type	(4) Separ. ($''$)	(5) r_{90}	(1) 1RXS J.....	(2) Name	(3) Type	(4) Separ. ($''$)	(5) r_{90}
162756.2+552239	PG 1626+554	Sy1	7.0	0.6	212124.3–665455	V390 Pav	K2Vp	6.3	0.5
162901.2+400753	EXO1627.3+4014	Sy1	5.5	0.5	213101.3+232009	LO Peg	K8	3.6	0.3
165352.6+394538	MRK 501	BL	5.0	0.5	213228.1+100812	II ZW 136	Sy1	8.3	0.7
165529.3–082008	V1054 Oph	M3Ve	6.1	0.5	214431.7+144612	HN Peg	G0V	11.7	0.7
165749.6+352022	HZ Her	LMXB	10.3	1.0	214702.5–160736	del Cap	A7IIIm	4.6	0.4
171734.5+102502	V2369 Oph	G5	2.7	0.2	214905.7–720603	AY Ind	M2Ve	19.3	1.5
171953.4+262958	GJ 669AB	dM4e+dM5e	10.9	0.9	215740.9–510027	GJ 841A	M0	7.0	0.5
172642.8+583726	PG 1725+587	DA1	7.3	0.7	215821.0+825218	V376 Cep	F5	3.8	0.4
173839.7+611410	HD 160934	K8V	1.7	0.2	215831.6–590043	BG Ind	F3V	13.1	1.0
175524.7+361122	V835 Her	G5	2.0	0.2	215852.2–301338	PKS 2155-304	BL	9.6	1.0
180009.9+683557	KUV 18004+6836	WD	4.0	0.4	220745.5–323519	A09.25	Sy1	17.7	1.5
180815.9+294127	V815 Her	G5	1.2	0.1	220907.9–274839	NGC 7214	Sy1	6.4	0.6
180921.5+295704	HD 166435	G0	4.1	0.4	221534.8–390053	CS Gru	G8+K0V	7.2	0.6
183355.9+514313	BY Dra	K6Ve	16.8	1.7	222329.1+322738	GJ 856A	M0Ve	10.7	0.9
184538.1–645144	CPD -64 3950	M0	11.7	0.8	222634.5–164433	HR 8545	G3V	5.4	0.5
191744.3–440021	HD 180235	K1+K2	13.5	1.0	223039.2–394246	PKS 2227-399	QSO	14.0	0.9
191812.8–382305	HD 180445	G8V	3.9	0.3	223845.5–203706	FK Aqr	M0Vpe	8.2	0.7
192129.2–345904	HR 7330	G5V	7.5	0.5	224441.6+175418	SAO 108142	K0	3.1	0.2
200925.6–484953	PKS 2005-489	BL	2.0	0.2	225624.2–313357	TW PsA	K4V	7.0	0.5
203719.4+753554	VW Cep	K0Vvar	5.8	0.6	225739.3–365607	MS 22549-3712	Sy1	4.8	0.4
204009.4–005216	AE Aqr	DQ	4.5	0.4	230028.2–334438	TZ PsA	G5Vp	8.9	0.7
204142.6–221910	GJ 1257	K5V	15.1	1.1	231221.6+104657	GD 246	DA1	9.6	0.7
204151.2–322604	AT Mic	M4Ve	4.4	0.4	232524.6–382653	IRAS23226-3843	Sy1	4.6	0.3
204509.4–312023	AU Mic	M0Ve	2.9	0.3	232750.2–861311	CPD -86 417	G5	5.7	0.5
204512.3–350953	BX Mic	G0V	8.1	0.7	233013.0–202324	GJ 1284	M2Ve	1.5	0.1
204606.2–251611	HR 7936	F5V	7.7	0.6	233231.1–121551	BPM 82931	M0	8.5	0.6
204744.8–363539	BO Mic	K0V	0.7	0.1	233246.5–164507	GJ 897AB	M3.5+?	10.5	0.9
210845.8–042539	SAO 145139	M1	6.8	0.5	233615.1–483502	CD -49 14193	K7	33.8	2.0
211123.3–522016	BR Ind	F8V	7.3	0.5	234244.1–143244	HR 8988	B9V	13.7	0.9
212050.3–530200	HD 202917	G5V	6.0	0.5	234328.8–145541	MS 23409-1511	QSO	11.1	0.8
					235503.5+283802	II Peg	K0V	1.9	0.2
					235728.4–302739	AM 2354-304	Sy1.2:	21.5	1.6

Notes:

1RXS J035025.0+171455 (V471 Tau): HR1= -0.7, white dwarf companion (Werner & Rauch 1997 and references therein)
1RXS J041521.5–073843 (40 Eri): HR1= -0.3, white dwarf companion
1RXS J132511.6–110932 (Spica): HR1= -0.9, coronal emission (Cassinelli et al. 1994)

class of the optical counterpart can be secured also by other means. This is the case for four sources classified as stars which are bright (one is nearby, parallax from TYCHO, the other three are very red objects on the POSS plates), two sources classified as supersoft X-ray sources, six galaxies which are presumed to have Seyfert Nuclei since they are bright X-ray sources, and six objects which coincide with radio sources and have the appropriate optical brightness to allow a classification as BL Lacs. The two supersoft sources (RX J054959.9–715158, situated in the LMC, and RX J134210.2+282250) entered X-ray low states after the RASS which prevented a more accurate localisation and optical identification in the dense star fields. For the extragalactic objects, determination of redshifts must await optical spectroscopy.

3.3. The content

Table 1 summarizes the results of the identification program. Normal stars, i.e. coronal emitters, are the most frequent counterparts of the known sources but are scarce among the new identifications. This is because the optical counterparts are mostly bright stars which were previously catalogued although this does not imply they were known as X-ray sources. Only 13 coronal sources coincide with stars which were not previously catalogued. The white dwarfs were also for a substantial part catalogued as such; they are included in the known subclass although they were not known as X-ray sources before the RASS. One nucleus of a planetary nebula is included in this subclass. The discovery power of X-ray observations is exemplified by the detection of extremely soft X-ray emission associated with

Table 3. Summary of the optical identification program for new sources in our sample ($|\,b\,| > 20°$, CR $> 0.5\,\mathrm{cts\,s^{-1}}$, and HR1 < 0). Columns denote (1) the name in the RASS BSC derived from the epoch-2000 X-ray position, (2) and (3) RA (2000) and DEC (2000) of the optical counterpart, (4) the separation between optical and X-ray positions in arcsec and (5) in units of the 90% confidence radii according to Eq. 2, (6) the RASS BSC PSPC count-rate CR in $\mathrm{cts\,s^{-1}}$, (7) the hardness ratio HR1, (8) the class and (9) the type of the optical counterpart, (10) the redshift z if extragalactic, (11) the visual magnitude V, and (12) the references to notes at the end of the table. Errors to CR and HR1 are given in brackets and refer to the last digits.

(1) 1RXS J.....	(2) RA,DEC(2000)	(3)	(4) Separation ($''$)	(5) r_{90}	(6) CR	(7) HR1	(8) Class	(9) Type	(10) z	(11) V	(12) Notes
001411.8–502243	0 14 11.0	–50 22 36	10.4	0.6	0.78 (08)	–0.10 (10)	AGN	BL:		18.5	1
001950.0+215651	0 19 49.9	21 56 53	2.4	0.2	2.00 (08)	–1.00 (01)	CV	SSS		12.4	1,8
002636.3–460101	0 26 35.4	–46 1 11	13.7	0.9	0.89 (08)	–0.46 (07)	AGN	BL		17.8	1,6
002958.0–632500	0 29 56.5	–63 24 57	9.2	0.7	3.11 (19)	–1.00 (01)	STAR	WD		15.0	1,2
003334.6–192130	0 33 34.2	–19 21 33	6.4	0.6	0.94 (06)	–0.22 (05)	AGN	BL		16.3	1,6
003915.6–511701	0 39 15.9	–51 17 0	3.0	0.2	0.96 (07)	–0.97 (01)	AGN	Sy1	0.029	15.3	1,4,8
010027.9–511346	1 0 27.1	–51 13 55	11.7	0.9	1.03 (07)	–0.22 (07)	AGN	Sy1	0.062	15.4	1,4
010538.7–141610	1 5 38.8	–14 16 14	4.3	0.3	1.49 (11)	–0.04 (07)	AGN				5
011730.7–382629	1 17 30.5	–38 26 30	2.6	0.2	0.93 (07)	–0.54 (07)	AGN	Sy1	0.225	16.5	1
012254.1–752117	1 22 53.0	–75 21 14	5.1	0.3	0.53 (07)	–0.99 (04)	CV	SSS		15.5	1,8
012806.9–184837	1 28 6.6	–18 48 31	7.4	0.6	0.74 (05)	–0.23 (06)	AGN			15.5	5
012910.8–214158	1 29 10.7	–21 41 57	1.7	0.1	0.86 (06)	–0.38 (06)	AGN	Sy1	0.093	15.4	1,4,6
014822.3–275828	1 48 22.2	–27 58 23	5.2	0.4	2.23 (14)	–0.59 (05)	AGN	Sy1	0.121	15.5	1,4
015227.1–231956	1 52 27.1	–23 19 54	2.0	0.2	1.05 (09)	–0.50 (07)	AGN	Sy1	0.113	15.6	1,4,6
020348.7+295921	2 3 48.6	29 59 26	5.2	0.4	0.54 (05)	–0.96 (03)	CV	AM		17.0	1,8
020922.2–522920	2 9 21.5	–52 29 21	6.5	0.6	0.77 (05)	–0.28 (06)	AGN	BL		16.9	1,6
022818.9–611817	2 28 19.2	–61 18 20	3.7	0.3	5.24 (23)	–0.99 (01)	STAR	F3IV+WD		8.8	2,8
024146.8–525943	2 41 46.6	–52 59 53	10.2	0.8	0.68 (07)	–0.12 (09)	STAR	dMe		10.7	2
025153.2+222735	2 51 53.8	22 27 35	8.3	0.7	0.97 (06)	–0.01 (06)	STAR	M:			5,8
031118.9–204621	3 11 18.7	–20 46 19	3.4	0.3	0.93 (07)	–0.05 (07)	AGN				5,6
031949.1–262719	3 19 48.7	–26 27 13	8.1	0.5	0.52 (06)	–0.49 (09)	AGN	Sy1	0.079	15.9	1,4
032315.7–493113	3 23 15.3	–49 31 7	7.2	0.6	1.31 (13)	–0.60 (07)	AGN	Sy1	0.071	16.5	1,4
034907.6–471107	3 49 7.6	–47 11 5	2.0	0.2	0.69 (04)	–0.76 (05)	AGN	Sy1	0.299	16.8	1,4
035629.1–364134	3 56 30.5	–36 41 20	21.9	0.4	0.70 (17)	–0.95 (12)	STAR	G2V+WD		12.5	8
041242.5–471238	4 12 41.4	–47 12 48	15.0	1.0	0.79 (09)	–0.49 (09)	AGN	Sy1	0.132	15.9	1,4
042601.6–571202	4 26 0.8	–57 12 1	6.6	0.5	4.56 (21)	–0.52 (08)	AGN	Sy1	0.104	14.1	1,4
042616.9–375730	4 26 17.1	–37 57 34	6.2	0.5	0.56 (06)	–0.03 (10)	STAR				5,8
043726.6–471118	4 37 28.1	–47 11 29	18.8	1.3	0.85 (09)	–0.64 (07)	AGN	Sy1	0.052	15.3	1,4
043939.4–531122	4 39 38.7	–53 11 31	11.0	0.7	0.76 (09)	–0.84 (05)	AGN	Sy1	0.243	16.2	1
043950.4–680854	4 39 49.6	–68 9 0	7.5	0.8	1.17 (03)	–0.99 (01)	CV	SSS		21.7	1,8
044307.1–034655	4 43 7.0	– 3 46 50	5.2	0.4	1.98 (18)	–1.00 (00)	STAR	WD		16.0	2
044723.1–275027	4 47 22.7	–27 50 38	12.2	1.1	0.82 (05)	–0.23 (06)	STAR	dMe		10.0	1,2
044924.2–435002	4 49 24.6	–43 50 8	7.4	0.6	0.91 (06)	–0.39 (06)	AGN	BL		15.0	1,6
045325.2–421335	4 53 25.5	–42 13 41	6.9	0.6	1.20 (08)	–1.00 (01)	CV	AM		19.0	1,2,8
045950.4–101544	4 59 50.4	–10 15 48	2.8	0.2	0.53 (04)	–0.35 (06)	STAR	G4V+WD		5.4	2,8
051206.1–004149	5 12 6.2	– 0 42 8	19.1	1.3	0.61 (04)	–1.00 (01)	STAR	WD		13.8	2
051223.5–414525	5 12 22.9	–41 45 28	7.4	0.6	0.71 (06)	–1.00 (01)	STAR	WD		16.5	2
051351.2–695145	5 13 50.8	–69 51 47	2.9	0.3	1.05 (03)	–0.87 (01)	CV	SSS		16.7	1,8
051723.3–352152	5 17 23.2	–35 21 52	1.2	0.1	0.61 (06)	–0.18 (10)	STAR	dMe		11.7	1,2
053136.3–462406	5 31 35.4	–46 24 8	9.5	0.7	0.73 (09)	–0.82 (06)	CV	AM		16.8	1,2,8
054959.9–715158					0.69 (02)	–0.64 (02)	CV	SSS			5,8
061549.4–582603	6 15 49.6	–58 26 5	2.5	0.2	0.66 (02)	–0.17 (03)	AGN				5
062555.6–600325	6 25 56.2	–60 3 29	6.0	0.5	0.54 (02)	–0.11 (04)	STAR	dMe		12.9	1
071506.6–702540	7 15 17.1	–70 25 8	61.7	4.2	2.24 (25)	–1.00 (01)	STAR	WD		14.5	1,2
074912.9–764202	7 49 13.7	–76 42 2	2.8	0.2	0.59 (07)	–0.22 (11)	STAR	dMe		11.7	1,2
081742.4–824331	8 17 40.4	–82 43 33	4.3	0.4	0.79 (05)	–0.21 (06)	STAR	dMe		10.9	1
084104.2+032118	8 41 3.7	3 21 17	7.6	0.7	1.21 (07)	–1.00 (01)	STAR	WD		15.0	2

Table 3. (continued)

(1) 1RXS J.....	(2) RA,DEC(2000)	(3)	(4) Separation ($''$)	(5) r_{90}	(6) CR	(7) HR1	(8) Class	(9) Type	(10) z	(11) V	(12) Notes
085902.0+484611	8 59 2.9	48 46 8	9.4	0.8	0.65 (04)	–0.13 (07)	AGN	Sy1	0.083		1
090233.6–065957	9 2 33.5	– 7 0 5	8.1	0.6	0.60 (05)	–0.20 (07)	AGN	Sy1	0.089		1
091003.8+353341	9 10 3.8	35 33 40	1.0	0.1	0.59 (04)	–0.01 (06)	STAR	M:			5,8
091657.6–194613	9 16 57.6	–19 46 21	8.0	0.6	0.96 (07)	–0.99 (02)	STAR	WD		17.3	2
091744.5+461229	9 17 45.2	46 12 26	7.9	0.7	0.69 (05)	–0.15 (07)	STAR	dMe		11.1	1
095752.3+852935	9 57 55.8	85 29 42	8.1	0.7	0.54 (03)	–1.00 (00)	STAR	WD		16.4	2
100211.4–192534	10 2 11.5	–19 25 36	2.4	0.2	0.60 (07)	–0.95 (03)	CV	AM		17.0	1,8
100542.2+433244	10 5 41.9	43 32 41	4.4	0.4	0.66 (04)	–0.61 (04)	AGN	Sy1	0.178	16.4	1,3,4
100710.1+220312	10 7 10.2	22 3 12	1.4	0.1	0.62 (04)	–0.06 (06)	AGN	Sy1	0.083	17.0	1
100734.4–201731	10 7 34.5	–20 17 32	1.7	0.1	1.00 (09)	–0.98 (03)	CV	AM		18.0	1,8
101534.8+090448	10 15 34.7	9 4 43	5.2	0.4	1.15 (10)	–0.85 (04)	CV	AM		16.5	1,8
101628.3–052026	10 16 28.6	– 5 20 34	9.2	0.7	3.96 (29)	–1.00 (01)	STAR	dM+WD		14.3	2,8
101900.8+375250	10 19 0.5	37 52 41	9.7	0.8	0.78 (04)	–0.07 (05)	QSO				3,6
103118.6+505341	10 31 18.4	50 53 37	4.4	0.4	4.46 (09)	–0.26 (02)	AGN	BL	0.239:	17.0	6,8
103210.2+532941	10 32 10.2	53 29 36	5.0	0.5	5.07 (10)	–1.00 (00)	STAR	WD		14.5	2,3
104311.5+490227	10 43 11.5	49 2 24	3.0	0.3	0.93 (04)	–1.00 (00)	STAR	WD		16.1	2,3
105916.6+512452	10 59 16.3	51 24 43	9.4	0.9	4.18 (09)	–0.99 (00)	STAR	WD		16.8	2,3
110021.3+401933	11 0 21.1	40 19 28	5.5	0.5	0.61 (04)	–0.35 (06)	AGN	BL:		17.3	5,6
111706.3+201410	11 17 6.2	20 14 7	3.3	0.3	4.34 (12)	–0.01 (02)	AGN	BL			3,6,8
111710.2+652211	11 17 10.0	65 22 7	4.2	0.4	0.55 (03)	–0.72 (03)	AGN	Sy1	0.147	16.4	1,3,4
112327.0+450715	11 23 27.3	45 7 14	3.3	0.3	0.55 (04)	–0.04 (07)	STAR	M:			5,8
114955.5+284510	11 49 55.7	28 45 8	3.3	0.3	3.34 (16)	–0.98 (01)	CV	AM		16.5	1,2,8
123137.5+704417	12 31 36.5	70 44 14	5.8	0.6	1.07 (04)	–0.17 (03)	AGN	Sy1	0.208	16.0	1,4
123651.1+453907	12 36 51.0	45 39 03	4.1	0.4	0.53 (04)	–0.27 (06)	AGN	Sy1.5	0.029	15.2	1,6
130255.6+505621	13 2 55.2	50 56 19	4.3	0.4	0.52 (03)	–0.05 (06)	AGN	BL:			5,6
130417.2+020539	13 4 17.0	2 5 36	4.2	0.3	0.69 (05)	–0.64 (05)	AGN	Sy1	0.229	17.1	8
130753.6+535137	13 7 53.9	53 51 30	7.5	0.7	1.86 (06)	–0.90 (01)	CV	AM		17.0	2,8
131317.1–325909	13 13 17.1	–32 59 12	3.0	0.2	2.16 (12)	–0.96 (02)	CV	AM		16.0	1,8
131422.6+342941	13 14 22.6	34 29 40	1.0	0.1	0.65 (04)	–0.63 (04)	AGN	Sy1	0.075	16.3	1,4
131931.7+140524	13 19 31.8	14 5 33	9.1	0.7	0.61 (06)	–0.25 (09)	AGN	BL			1,6
131957.2+523533	13 19 57.0	52 35 33	1.8	0.2	0.66 (04)	–0.52 (05)	QSO				3,6
132046.7+070130	13 20 47.2	7 1 24	9.6	0.8	0.76 (05)	–0.22 (06)	STAR	K			1,2
133241.6+223007	13 32 42.2	22 30 11	9.2	0.8	0.84 (05)	–0.13 (05)	STAR	dKe		9.6	2
134210.2+282250					0.57 (04)	–0.95 (02)	CV	SSS			5,8
135515.9+561244	13 55 16.5	56 12 45	5.1	0.4	0.55 (06)	–0.55 (08)	AGN	Sy1	0.122	16.5	1,3,4,6
141336.8+702954	14 13 36.7	70 29 51	3.0	0.3	0.63 (04)	–0.07 (06)	AGN	Sy1	0.107	16.9	1,4
143917.7+393248	14 39 17.4	39 32 43	6.1	0.6	1.43 (05)	–0.35 (03)	AGN	BL		16.0	6,8
144801.0+360833	14 48 0.6	36 8 31	5.2	0.4	0.60 (04)	–0.54 (05)	AGN	BL:			5,6
152907.5+561604	15 29 7.4	56 16 6	2.2	0.2	0.74 (03)	–0.43 (03)	AGN	Sy1	0.099		3,6
160518.5+542101	16 5 19.0	54 20 59	4.8	0.4	0.50 (02)	–0.11 (04)	STAR	M			3
160518.8+324907					0.87 (04)	–0.70 (03)					7
161809.2+361951	16 18 9.4	36 19 57	6.5	0.7	0.85 (03)	–0.43 (03)	AGN	Sy1	0.034	16.6	1,3,4
161951.7+405834	16 19 51.3	40 58 46	12.8	1.1	0.51 (03)	–0.54 (04)	AGN			16.0	3
162456.7+755457	16 24 56.6	75 54 56	1.1	0.1	0.54 (02)	–0.20 (04)	AGN	BL:			1
162909.4+780439	16 29 11.1	78 4 41	5.6	0.6	5.66 (07)	–0.99 (00)	STAR	dMe+WD		13.0	2,8
163124.7+421656	16 31 24.7	42 17 2	6.0	0.5	0.53 (03)	–0.07 (04)	AGN	BL:		19.8	5,6
170231.2+324722	17 2 31.0	32 47 20	3.2	0.3	0.56 (03)	–0.46 (04)	AGN	Sy1	0.164		3,6
171304.5+352335	17 13 4.5	35 23 34	1.0	0.1	0.99 (04)	–0.15 (03)	AGN	BL:			5,6
174614.9–703902	17 46 13.2	–70 38 56	10.4	0.8	1.08 (09)	–1.00 (02)	STAR	WD		16.0	1,2
182030.0+580437	18 20 29.7	58 4 41	4.7	0.5	0.87 (02)	–1.00 (00)	STAR	WD		13.8	2
184449.1–741840	18 44 47.8	–74 18 33	8.8	0.5	0.94 (08)	–0.61 (06)	CV	AM		17.6	1,2,8
192558.3–563344	19 25 58.6	–56 33 36	8.4	0.4	6.86 (58)	–0.98 (02)	STAR	G+WD			1,2,8
193835.9–461256	19 38 35.6	–46 12 57	3.3	0.3	5.32 (25)	–1.00 (01)	CV	AM		15.5	1,2,8
195711.1–573823	19 57 11.5	–57 38 22	3.4	0.3	0.90 (07)	–0.94 (02)	CV	AM		18.0	1,8

Table 3. (continued)

(1) 1RXS J.....	(2)	(3) RA,DEC(2000)	(4) Separation ($''$)	(5) r_{90}	(6) CR	(7) HR1	(8) Class	(9) Type	(10) z	(11) V	(12) Notes
200905.6–602537	20 9 5.1	–60 25 42	6.2	0.6	8.65 (19)	–1.00 (00)	STAR	WD		13.4	2
210758.5–051744	21 7 58.2	– 5 17 39	6.7	0.5	0.81 (06)	–1.00 (02)	CV	AM		15.3	1,2,8
212529.0–813836	21 25 24.6	–81 38 27	13.2	1.0	0.69 (07)	–0.14 (09)	STAR	dMe		9.4	1
212626.8+192224	21 26 26.5	19 22 32	9.1	0.7	1.05 (07)	–1.00 (00)	STAR	A8m+WD		6.1	2,8
214636.3–305132	21 46 35.8	–30 51 42	11.9	0.9	0.84 (07)	–0.13 (10)	AGN				5,6
215621.5–543820	21 56 21.0	–54 38 24	5.9	0.5	5.94 (31)	–1.00 (01)	STAR	WD		14.3	2
215635.1–414220	21 56 35.1	–41 42 19	1.0	0.1	0.99 (08)	–1.00 (01)	STAR	WD		15.7	2
221653.7–445154	22 16 53.0	–44 51 57	8.0	0.7	1.30 (09)	–0.64 (05)	AGN	Sy1	0.136	15.8	1,4
221757.1–594134	22 17 56.6	–59 41 31	4.8	0.4	0.80 (05)	–0.67 (04)	AGN	Sy1	0.160	16.2	1,4
222129.6–522530	22 21 29.3	–52 25 27	4.1	0.3	0.54 (04)	–0.35 (06)	AGN	BL		16.9	1,6
224237.9–384520	22 42 37.6	–38 45 17	4.6	0.3	0.65 (05)	–0.71 (05)	AGN	Sy1	0.221	16.9	1,4
224250.9–714222	22 42 48.4	–71 42 22	11.8	0.8	0.73 (08)	–0.21 (10)	STAR	dK5e		11.5	1
224457.7–331506	22 44 57.6	–33 14 59	7.1	0.5	1.05 (06)	–0.23 (05)	STAR	dMe		13.0	1
224520.3–465212	22 45 20.3	–46 52 12	0.0	0.0	1.54 (12)	–0.68 (05)	AGN	Sy1	0.201	14.8	1,4
224841.4–510951	22 48 40.8	–51 9 53	6.0	0.5	2.24 (17)	–0.65 (05)	AGN	Sy1	0.102	15.5	1,2,4
225845.8–260917	22 58 45.3	–26 9 15	7.0	0.5	0.66 (08)	–0.16 (12)	AGN	Sy1	0.076	16.1	1,4
230136.8–591325	23 1 36.2	–59 13 19	7.6	0.6	0.86 (07)	–0.07 (08)	AGN				5
230152.0–550827	23 1 52.0	–55 8 31	4.0	0.3	0.79 (07)	–0.70 (06)	AGN	Sy1	0.140	15.4	1,4
230437.5–350114	23 4 37.3	–35 1 13	2.7	0.2	0.55 (07)	–0.39 (10)	AGN	Sy1	0.042	16.6	1,4
231235.4–340426	23 12 34.5	–34 4 21	12.2	0.7	0.54 (07)	–0.11 (12)	AGN	BL:			5,6
231603.9–052713	23 16 3.4	– 5 27 9	8.5	0.7	1.10 (09)	–0.96 (02)	CV	AM		18.0	1,8
231749.8–442230	23 17 49.9	–44 22 27	3.2	0.2	0.71 (06)	–0.77 (05)	AGN	Sy1	0.134	16.8	1,4
232431.0–544148	23 24 30.9	–54 41 36	12.0	0.9	1.33 (10)	–1.00 (02)	STAR	WD		15.2	1,2
232444.9–404053	23 24 44.5	–40 40 51	5.0	0.3	1.46 (11)	–0.34 (07)	AGN	BL		15.5	1
232512.2–323637	23 25 11.6	–32 36 35	7.8	0.5	0.54 (08)	–0.63 (12)	AGN	Sy1	0.216	17.0	1,4
234923.9–312602	23 49 23.9	–31 26 3	1.0	0.1	0.63 (05)	–0.52 (06)	AGN	Sy1	0.135	16.6	1,4

Notes:

1: spectroscopic identification, this work
2: WFC identification (Pye et al. 1995, Mason et al. 1995)
3: Hamburg/RASS identification (Bade et al. 1998)
4: Grupe et al. 1998
5: inferred identification from the Digitized Sky Survey (see Sect. 3.2)
6: radio source (see Sect. 3.2)
7: blank field
8: Remarks to individual sources

1RXS J001950.0+215651: Galactic supersoft X-ray source (Beuermann et al. 1995), new name QR And
1RXS J003915.6-511701: WPVS007, Grupe et al. 1995b
1RXS J012254.1–752117: PG1159 star (Cowley et al. 1995)
1RXS J020348.7+295921: AM Herculis binary (Schwarz et al., in preparation)
1RXS J022818.9–611817: White dwarf companion (Landsman et al. 1993)
1RXS J025153.2+222735: bright red star
1RXS J035629.1–364134: White dwarf companion (Christian et al. 1996)
1RXS J042616.9–375730: nearby star (T7578 425 1)
1RXS J043950.4–680854: Supersoft X-ray source in the LMC (van Teeseling et al. 1996)
1RXS J045325.1–421335: AM Herculis binary (Burwitz et al. 1996), new name: RS Cae
1RXS J045950.4–101544: White dwarf companion (Landsmann et al. 1993)
1RXS J051351.2–695145: Supersoft X-ray source in the LMC (Pakull et al. 1993)
1RXS J053136.3–462406: AM Herculis binary (Reinsch et al. 1994), new name UW Pic
1RXS J054959.9–715158: Supersoft X-ray source in the LMC (Cowley et al. 1993, Reinsch et al. 1996b)
1RXS J091003.8+353341: bright red star
1RXS J100211.4–192534: AM Herculis binary (Beuermann & Thomas 1993)

Table 3. (continued) **Notes:**

1RXS J100734.4–201731: AM Herculis binary (Beuermann & Thomas 1993)
1RXS J101534.8+090448: AM Herculis binary (Burwitz et al. 1998)
1RXS J101628.3–052026: White dwarf companion (Tweedy et al. 1993)
1RXS J103118.6+505341: Identified by Bade et al. (1994)
1RXS J111706.3+201410: Identified by Brinkmann et al. (1997)
1RXS J112327.0+450715: bright red star
1RXS J114955.5+284510: AM Herculis binary (Mittaz et al. 1992), new name EU UMa
1RXS J130417.2+020539: Identified by Miller et al. (1998, in prep.)
1RXS J130753.6+535137: AM Herculis binary (Osborne et al. 1994)
1RXS J131317.1–325909: AM Herculis binary (Beuermann & Thomas 1993)
1RXS J134210.2+282250: Supersoft X-ray source (Hertz et al. 1993)
1RXS J143917.7+393248: Identified by Fleming et al. (1993)
1RXS J162909.4+780439: White dwarf companion (Cooke et al. 1992)
1RXS J184449.1–741840: AM Herculis binary (O'Donoghue et al. 1993), new name V347 Pav
1RXS J192558.3–563344: White dwarf companion (Barstow et al. 1994)
1RXS J193835.9–461256: AM Herculis binary (Buckley et al. 1993), new name QS Tel
1RXS J195711.1–573823: AM Herculis binary (Thomas et al. 1996)
1RXS J210758.5–051744: AM Herculis binary (Hakala et al. 1993, Schwope et al. 1993), new name HU Aqr
1RXS J212626.8+192224: White dwarf companion (Wonnacott et al. 1993)
1RXS J231603.9–052713: AM Herculis binary (Beuermann & Thomas 1993)

normal stars. Nine stars of spectral types A$-$M (three in Table 2 and six in Table 3) with visual magnitudes between 6.1 and 14.3 have HR1 $= -1.0$. For comparison, the mean hardness ratio of A$-$M stars in this soft X-ray selected sample is HR1 $= -0.15$ with a standard distribution of 0.11. It is extremely unlikely that the very soft X-ray emission in all nine stars is of coronal origin and the likely explanation is that they are binaries containing a hot white dwarf which in the optical is outshone by the normal star. Two of these objects (RX J043746.1–011930 = StHA 32 and RX J160141.2+664811 = AG Dra) are well-studied symbiotic stars (Schmid & Nussbaumer 1993), one is known to contain a possible white-dwarf companion to HD 74389 (Sanduleak & Pesch 1990, Liebert et al. 1990), in the remaining six objects the white-dwarf companions have been detected by follow-up observations after the RASS (for references see Table 3). Three more sources are known to contain a white dwarf, these are RX J035025.0+171455 = V471 Tau, RX J041521.5–073843 = 40 Eri, and RX J045950.4–101544 (Landsmann et al. 1993).

The largest increase percentagewise is found for cataclysmic variables, i.e. accreting white dwarfs in close binaries. Without exception, the 14 newly discovered CVs belong to the subclass of AM Herculis binaries which contain a magnetic white dwarf; these objects are known to be spectacular soft X-ray sources. Only 18 AM Herculis binaries were known in pre-ROSAT times (Ritter 1990), of these 12 at latitudes $|\,b\,| > 20°$. Of these 12 again only 4 were sufficiently X-ray bright during the RASS to be detected with CR $> 0.5\,\mathrm{cts\,s^{-1}}$ (a fifth, UZ For, happened to lie in the small section of the sky not covered in the initial RASS). The other 3 known sources in line 4 of Table 1 are: HZ Her (LMXB), Cal 83 (supersoft source), and AE Aqr (IP). The remaining 6 new objects are all supersoft sources.

Among the newly identified X-ray sources AGN represent the largest fraction with 41 Seyfert galaxies and quasars as well as 12 BL Lac objects. AGN are characterized by high X-ray vs. optical flux ratios which implies that these systems are optically less conspicuous than the coronally emitting stars; consequently they had a much higher chance of not being catalogued previously. The number of AGN among the bright soft RASS sources increased, therefore, substantially, namely by 60%. All spectroscopically identified Seyfert galaxies and quasars are fairly nearby with redshifts ranging from $z = 0.029$ to $z = 0.299$. Their mean count-rate and redshift values are $\overline{CR} = 1.0\,\mathrm{cts\,s^{-1}}$ and $\bar{z} = 0.12$, respectively. For comparison, the Seyferts and quasars in the known subsample have $\overline{CR} = 1.6\,\mathrm{cts\,s^{-1}}$ and $\bar{z} = 0.09$. Not surprisingly, the new systems are typically more distant than the previously known ones. A comparison is also of interest with the corresponding numbers for the subclass of hard X-ray sources (HR1 > 0) not considered in this paper. For simplicity, we restrict the comparison to the X-ray brightest AGN with PSPC count-rates CR $> 1\,\mathrm{cts\,s^{-1}}$. Above this limit, the RASS contains 35 previously known Seyfert galaxies and quasars with X-ray hard spectra (HR1 > 0) which have a mean count-rate $\overline{CR} = 2.1\,\mathrm{cts\,s^{-1}}$ and a mean redshift $\bar{z} = 0.05$. For comparison, Table 2 contains 28 soft Seyfert galaxies above $1\,\mathrm{cts\,s^{-1}}$ with mean values $\overline{CR} = 2.6\,\mathrm{cts\,s^{-1}}$ and $\bar{z} = 0.05$. As $\overline{CR}$ and $\bar{z}$ are about the same for the brightest hard and soft Seyferts and the conversion factor from count-rate to energy flux in the ROSAT band varies only slowly with spectral index, both spectral subsamples reach about the same luminosities and contribute about equally to the X-ray luninosity function of Seyfert galaxies and quasars.

As we are dealing here with the brightest sources in the RASS, many of the newly identified sources turned out to be highly interesting objects for which follow-up observations were immediately initiated (e.g. Beuermann et al. 1995, Burwitz et al. 1996, 1998, Grupe et al. 1995a, 1995b, Reinsch et al.

1994, Shafter et al. 1996, Schwope et al. 1993, 1995, Thomas et al. 1996, van Teeseling et al. 1996, Trümper et al. 1991, see also the notes appended to Table 3).

Taken together, the results of this program have provided us with a substantial number of new identifications of bright soft RASS sources yielding important progress in our understanding of several classes of soft X-ray emitters. Discussions of the properties of individual sources and of subclasses of sources are given in separate papers, e.g. for AGN (Grupe et al. 1998), supersoft X-ray binaries (Beuermann et al. 1995, van Teeseling et al. 1996, Reinsch et al. 1996a, 1996b) and cataclysmic variables (Beuermann & Thomas 1993, Beuermann & Burwitz 1995, see also the references given in the Introduction and in the notes appended to Table 3).

Acknowledgements. The ROSAT project is supported by the Bundesministerium für Bildung, Wissenschaft, Forschung und Technologie (BMBF/DLR) and the Max-Planck-Gesellschaft. We thank the ROSAT team for performing the All-Sky Survey and producing the RASS Bright Source Catalogue. We also thank the optical observers Drs. Frederic Hessman and Dirk Grupe who contributed to the identification program. This research has made use of the SIMBAD database operated at CDS, Strasbourg, France, and the NASA/IPAC Extragalactic Database (NED) operated by the Jet Propulsion Laboratory, California Institute of Technology under contract with the National Aeronautics and Space Asministration. Identification of the RASS X-ray sources was greatly facilitated by use of the finding charts based upon the COSMOS scans of the ESO/SERC J plates performed at the Royal Observatory Edinburg and APM catalogue based on scans of the red and blue POSS plates performed at the Institute of Astronomy, Cambridge, UK. This work has also been supported in part by the DLR under grant 50 OR 9403 5.

References

Bade N., Engels D., Voges W. et al. 1997, A&AS 127, 145
Bade N., Fink H.H., Engels D. 1994, A&A 286, 381
Barstow M.A., Holberg J.B., Fleming T.A. et al. 1994, MNRAS 270, 499
Beuermann K., Burwitz V. 1995. In: Buckley D., Warner B. (eds.) Magnetic Cataclysmic Variables. ASP Conf. Ser. 85, 99
Beuermann K., Reinsch K., Barwig H. et al. 1995, A&A 294, L1
Beuermann K., Thomas H.-C. 1993, Adv. Space Res. 13(12), 115
Brinkmann W., Siebert J., Feigelson E.D. et al. 1997, A&A 323, 739
Buckley D.A.H., O'Donoghue D., Hassall B.J.M. et al. 1993, MNRAS 262, 93
Burg R., Giacconi R., Huchra J. et al. 1992, A&A 259, L9
Burwitz V., Reinsch K., Schwope A.D. et al. 1996, A&A 305, 507
Burwitz V., Reinsch K., Schwope A.D. et al. 1998, A&A 331, 262
Cassinelli J.P., Cohen D.H., MacFarlane J.J. et al. 1994, ApJ 421, 705
Christian D.J., Vennes S., Thorstensen J.R., Mathioudakis M. 1996, AJ 122, 258
Cooke B.A., Barstow M.A., Breeveld E.R. et al. 1992, Nat 355, 61
Cowley A.P., Schmidtke P.C., Hutchings J.B., Crampton D. 1995, PASP 107, 927
Cowley A.P., Schmidtke P.C., Hutchings J.B. et al. 1993, ApJ 418, L63
Ebeling H., Voges W., Böhringer H., Edge A.C. 1993, A&A 275, 360
Fleming T.A., Green R.F., Jannuzi B.T. et al. 1993, AJ 106, 1729
Grupe D., Beuermann K., Mannheim K. et al. 1995a, A&A 299, L5
Grupe D., Beuermann K., Mannheim K. et al. 1995b, A&A 300, L21
Grupe D., Beuermann K., Thomas H.-C. et al. 1998, A&A 330, 25
Hakala P.J., Watson M.G., Vilhu O. et al. 1993, MNRAS 263, 61
Hasinger G., Burg R., Giacconi R. et al. 1993, A&A 275, 1
Hasinger G., Fischer J.-U., Schwope A.D. et al. 1997, Astron. Nachr. 318, 329
Hertz P., Grindlay J.E., Bailyn C.D. 1993, ApJ 410, L87
Landsman W., Simon T., Bergeron P. 1993, PASP 105, 841
Liebert J., Bergeron P., Saffer R.A. 1990, PASP 102, 1126
Mason K.O., Hassall B.J.M., Bromage G.E. et al. 1995, MNRAS 274, 1194
McMahon R.G., Irwin M.J. 1992. In: MacGillivray H.T., Thomson E.B. (eds.) Digitised Optical Sky Surveys. Kluwer, Dordrecht, p. 417
Mittaz J.P.D., Rosen S.R., Mason K.O., Howell S.B. 1992, MNRAS 258, 277
Motch C., Guillot P., Haberl F. et al. 1997a, A&A 318, 111
Motch C., Guillot P., Haberl F. et al. 1997b, A&AS 122, 201
Nugent J.J., Jensen K.A., Nousek J.A. et al. 1983, ApJS 51, 1
O'Donoghue D., Mason K.O., Chen A. et al. 1993, MNRAS 265, 545
Osborne J.P., Beardmore A.P., Wheatley P.J. et al. 1994, MNRAS 270, 650
Pakull M.W., Motch C., Bianchi L. et al. 1993, A&A 278, L39
Pfeffermann E., Briel U.G., Hippmann H. et al. 1986, SPIE 733, 519
Pounds K.A., Allan D.J., Barber C. et al. 1993, MNRAS 260, 77
Pye J.P., McGale P.A., Allan D.J. et al. 1995, MNRAS 274, 1165
Reinsch K., Burwitz V., Beuermann K., Schwope A.D., Thomas H.-C. 1994, A&A 291, L27
Reinsch K., van Teeseling A., Beuermann K., Abbott T.M.C. 1996a, A&A 309, L11
Reinsch K., van Teeseling A., Beuermann K., Thomas H.-C. 1996b. In: Greiner J. (ed.) Supersoft X-Ray Sources. Springer, Berlin, p. 173
Ritter H. 1990, A&AS 85, 1179
Sanduleak N., Pesch P. 1990, PASP 102, 440
Schwope A.D., Thomas H.-C., Beuermann K. 1993, A&A 271, L25
Schwope A.D., Thomas H.-C., Beuermann K. et al. 1995, A&A 293, 764
Schmid H.M., Nussbaumer H. 1993, A&A 268, 159
Shafter A.W., Reinsch K., Beuermann K. et al. 1996, ApJ 443, 319
Thomas H.-C., Beuermann K., Reinsch K., Schwope A.D. 1996, A&A 313, 833
Trümper J., Hasinger G., Aschenbach B. et al. 1991, Nature 349, 579
Tweedy R.W., Holberg J.B., Barstow M.A. et al. 1993, AJ 105, 1938
van Teeseling A., Reinsch K., Beuermann K. 1996, A&A 307, L49
Veron-Cetty M.P., Veron P. 1996, ESO SR 17, 1
Voges W. 1997, The All-Sky Survey and Pointing Catalogues of ROSAT. In: Di Gesu' V., Duff M.J.B., Heck A. et al. (eds.) Data Analysis in Astronomy V. World Sci. Publ., Singapore, p. 189
Voges W., Aschenbach B., Boller Th. et al. 1996a, IAU Circ. 6420
Voges W., Aschenbach B., Boller Th. et al. 1998, to be published in A&AS
Voges W., Boller T., Dennerl K. et al. 1996b. In: Zimmermann H.U., Trümper J., Yorke H., Röntgenstrahlung from the Universe. MPE Report 263, p. 637
Wamsteker W., Pieto, A. Vitores A. et al. 1985, A&AS 62, 255
Werner K., Rauch T. 1997, A&AS 324, L25
Wonnacott D., Kellett B.J., Stickland D.J. 1993, MNRAS 262, 277
Yentis D.J., Cruddace R.G., Gursky H. et al. 1992. In: MacGillivray H.T., Thomson E.B. (eds.) Digitised Optical Sky Surveys. Kluwer, Dordrecht, p. 67
Zickgraf F.-J., Thiering I., Krautter J. et al. 1997, A&AS 123, 103